

Phase morphology development in immiscible PP/(PS/PPE) blends influence of the melt-viscosity ratio and blend composition

V. Everaert^a, L. Aerts^b, G. Groeninckx^{a,*}

^aCatholic University of Leuven, Department of Chemistry, Laboratory for Macromolecular Structural Chemistry, Celestijnenlaan 200F, B-3001 Heverlee, Belgium

^bDow Benelux N.V., PO Box 48, 4530 Terneuzen, The Netherlands

Received 2 October 1998; accepted 5 January 1999

Abstract

Immiscible blends of isotactic polypropylene (PP) with a miscible amorphous phase containing varying concentrations of polystyrene (PS) and poly (2,6-dimethyl-1,4-phenylene ether) (PPE) were prepared in the melt, to study the influence of the blend composition and the melt-viscosity ratio, p , on the phase morphology. This model blend system offers the unique opportunity to vary the composition of the miscible amorphous PS/PPE phase, without affecting the global interfacial tension, a crucial parameter with respect to phase morphology development. All immiscible PP/(PS/PPE) blends were prepared in a co-rotating twin-screw mini-extruder under constant processing conditions. The location of the phase inversion region was strongly related to the viscosity ratio. A composite-like morphology was observed in this region. To be able to separate the effects of droplet break-up and coalescence with respect to particle size, blends containing only 1 wt.% dispersed phase were investigated over a viscosity ratio range from 0.05 to 20. The results showed a clear dependence of the blend phase morphology on the viscosity ratio; highly viscous matrices ($p \ll 1$) enhance droplet break-up due to their efficient shear stress transfer towards the dispersed phase and the higher dispersive forces acting on it; low viscous matrices ($p > 1$) often act as a lubricant for the dispersed phase reducing droplet break-up. The influence of the viscosity ratio on droplet break-up is reflected in the particle diameter in blends with a concentration of the dispersed phase up to 20 wt.%. In the latter case, blends with a low viscosity ratio ($p < 1$) offer the best approach towards a fine and stable phase morphology, unlike suggestions in the literature. Blends containing higher concentrations of the minor phase (>20 wt.%) exhibit strong coalescence during melt-mixing; the influence of the viscosity ratio on the final blend phase morphology becomes less obvious, and the finest dispersion was observed at $p = 1$. Only blends of a lower viscous matrix in which a highly viscous phase has to be dispersed, do not follow the previous tendency as a result of the strong impact of a changing overall melt-viscosity. A quiescent thermal treatment of the blends showed that the concentration of the dispersed phase is the most important factor determining phase coarsening in blends having nearly equal melt-viscosities. Blending a highly viscous component with a low viscous component seems to counteract quiescent phase coarsening. © 1999 Elsevier Science Ltd. All rights reserved.

Keywords: Phase morphology; Immiscible blends; Viscosity ratio

1. Introduction

Most properties of blends of immiscible polymers depend on the fineness of the phase morphology [1]. For this reason, it is very important to study the relationship between material characteristics (interfacial tension, melt-viscosity and melt-elasticity, molecular weight), processing conditions (time of mixing, temperature of mixing, screw speed, mixer type), blend composition and the final blend phase morphology. Development of the blend phase morphology during melt-mixing of immiscible polymers has been studied in many articles [2–25]. However, still

contradictory results are reported in the literature and the formulation of some general rules relating all the previously mentioned parameters with the final blend phase morphology is not yet possible [2]. As the industrial importance of immiscible polymer blends is increasing, still further, it is of crucial importance to understand in detail the fundamental parameters controlling the blend phase morphology during and after melt-processing.

The main mechanism governing phase morphology development in immiscible polymer blends is believed to be the result of both droplet break-up and coalescence [3–5]. Dispersed domains under shear flow will *break-up* as long as the shear forces applied by the flow field can overcome the interfacial forces. The minimum obtainable droplet diameter in immiscible blend systems can be

* Corresponding author.

estimated from the critical capillary number (Eq. 1),

$$(\text{Ca})_{\text{crit}} = \frac{\eta_m \dot{\gamma} r}{\sigma_{12}} \quad (1)$$

where η_m represents the matrix viscosity (Pa s), $\dot{\gamma}$ the shear rate (s^{-1}), r the average droplet radius (m) and σ_{12} the interfacial tension (N/m). If the capillary number (Ca) is larger than the critical capillary number $(\text{Ca})_{\text{crit}}$, droplets can further deform and break-up. Taylor [6] derived a function for the value of $(\text{Ca})_{\text{crit}}$ in the case of Newtonian systems under simple shear flow (Eq. 2)

$$(\text{Ca})_{\text{crit}} = \frac{1}{2} \frac{16p + 16}{19p + 16} \quad (2)$$

where p is the viscosity ratio η_d/η_m , with η_d being the viscosity of the dispersed phase (Pa s). As coalescence is not accounted for in this equation, it is often used as a lower limit for the minimum obtainable particle size (Taylor-limit). Experiments showed that this equation is only a good approximation in a limited range of viscosity ratios [7], i.e., $0.1 < p < 1$. An elongational flow field has proved to be more effective in deforming particles than a shear flow field [7].

Several authors have investigated the influence of the viscosity ratio on the final phase morphology of non-Newtonian melt-mixed blend systems. Based on the experimental data of PA/rubber blends with varying viscosity ratios and interfacial tensions. Wu [8] has established an empirical equation fitting the capillary master curve:

$$2\text{Ca} = \frac{\eta_m \dot{\gamma} D_n}{\sigma_{12}} = 4 \left(\frac{\eta_d}{\eta_m} \right) \pm 0.84 \quad (3)$$

In this equation, the exponent is positive for $p > 1$ and negative for $p < 1$; D_n represents the number average particle diameter. However, the blends investigated contained 15 wt.% of the dispersed phase, leading to an overestimation of the critical capillary number, $(\text{Ca})_{\text{crit}}$. In practice, it was shown that a dispersed phase concentration of 0.5 to 1 wt.% can already give rise to flow induced coalescence [9,10].

Coalescence is thus an important factor influencing the dispersed phase morphology. The course of coalescence in a quiescent molten polymer blend is often described as a four-step process [4,11]. The first step concerns the *approach* of the droplets as a result of the flow field or, in a quiescent melt, as the result of Brownian motions [12,13]; the higher the concentration of the dispersed phase, the closer the droplets and the higher the probability of collision. In practice, it is assumed that the first step is only important in systems with a volume fraction, ϕ , of the dispersed phase lower than 10%; for higher concentrations, many droplets practically touch each other because a system of spheres has its percolation threshold at $\phi = 15.6$ vol.% [14]. A second step required for coalescence is the *deformation* of droplets during collision along with the removal of the matrix film in between the droplets (*'film drainage'*). This step is often

considered as the rate-determining step for coalescence [5,11,50], and has been related to interface mobility and size of the droplets. The third step concerns the *rupture* of the remainder of the matrix film, at the thinnest spot, usually by the formation of a hole. Finally, the coalescing drops merge to form again one single droplet.

In general, coalescence during melt-mixing will be governed by the interfacial mobility, which is quite high for polymer melts [15]. As a result, a relatively high coalescence rate is encountered in polymer blends. However, the latter can be reduced if the matrix becomes highly viscous [9,16]. Moreover, it is reported that the contact time required for coalescence increases when the droplet diameter increases, or the density difference between droplets and matrix increases [9]. Fortelný et al. [2,17] proposed an equation taking into account both droplet break-up and coalescence to predict the final blend morphology equation (Eq. 4)

$$r = r_{\text{crit}} + \left(\frac{\sigma_{12}}{\eta_m} \frac{\alpha}{f_1} \right) \phi \quad (4)$$

where r_{crit} represents the critical droplet radius as calculated from $(\text{Ca})_{\text{crit}}$; α is the probability that droplets will coalesce after collision; f_1 is the slope of a function describing the frequency of droplet break-up at $(\text{Ca})_{\text{crit}}$ and is the volume fraction of the dispersed phase. This relationship still contains several parameters which cannot easily be quantified for the blending of viscoelastic polymers.

In practice, reported investigations on the influence of viscosity ratio and blend composition on the phase morphology development in immiscible polymer blends are often contradictory. Hietaoja et al. [18] found a linear increase in the particle size with increasing viscosity ratio for PA-66/PP blends with PA-66 as the dispersed phase, while no correlation was found when PP formed the dispersed phase. In contrary, Favis and Chalifoux [19,20] studied PP/PC blends and observed for viscosity ratios below 1, with PP as matrix, a minimum particle size at a viscosity ratio $p = 0.15$. Favis and Therrien [21] showed that phase structure formation is closely related to viscosity ratio, blend composition, and the type of mixing device. Blends prepared in an internal mixer showed to be always coarser than in a twin-screw extruder, and this phenomenon was most pronounced at high viscosity ratios. According to Plochocki et al. [22], the particle size as a function of mixing energy goes through a minimum, caused by the different influences of mixing conditions and the process of dispersion and coalescence. Vainio and Seppälä [23] stated that the shear stress would be a more important factor in controlling the phase morphology than the shear-rate dependent viscosity ratio. It was suggested that a high energy input can lead to more coalescence in the blend as collision forces would be much higher. However, Ghodgaonkar and Sundararaj [24] recently suggested that droplet elasticity could be responsible for this behaviour. Elastic droplets would resist deformation more easily at higher shear rates because droplet elasticity

Table 1
Basic material characteristics

Material	MFI (g/10 min)	M_n (GPC)	M_w (GPC)	Polydispersity	Density (g/cm ³)
PP12	12 (230°C)	46 400 ^a	260 000 ^a	5.6	0.91
PP40	40 (230°C)	50 200 ^a	215 000 ^a	4.3	0.91
PS	—	81 900 ^b	190 000 ^b	2.6	1.055
PPE	13 (300°C)	19 300 ^b	54 300 ^b	2.8	1.065

^a Measured in TCB at 140°C; molecular weights are based on polyethylene standards and multiplied with a factor 1.55 (calculated from the Mark-Houwink constants for PP and PE)¹. (Cf. Scholte et al., J Appl Polym Sci 1984;29).

^b Measured in THF at 25°C; molecular weights are based on polystyrene standards.

tends to have a stabilizing effect during deformation, causing the minimum attainable droplet diameter being larger when the medium is elastic. These authors proposed a new equation for the estimation of the droplet diameter in viscoelastic blends by balancing the droplet deforming forces (shear force and matrix elasticity) and deformation resisting forces (interfacial forces and droplet elasticity). Namhata et al. [25] developed a model to predict blend morphology development during melt-flow based on the fact that when two phases of different viscosities are subjected to a stress field, each phase will have a different velocity resulting in a difference in volumetric flow rate. These authors stated that the viscosity ratio should be determined at the same shear stress instead of using a viscosity ratio criterion based on viscosities measured at the same shear rate.

The aim of the present article is to investigate in detail the blend phase morphology and the coalescence rate during a quiescent thermal treatment as a function of viscosity ratio, melt elasticity and blend composition [26] in immiscible PP/(PS/PPE) blends. This model blend system offers the unique advantage that a variation in the miscible PS/PPE composition allows to vary the viscosity ratio and melt-elasticity of the phases, without affecting the interfacial tension, a crucial parameter with respect to phase morphology development [27,28]. Until now, most of the investigations with respect to the influence of the viscosity ratio have been performed by varying the molecular weight of one or both components, without taking into account that the latter can have an influence on the interfacial tension in the blend system.

Table 2
Miscible amorphous PS/PPE phases

Blend composition	Code name	T_g (DSC) (°C)	T_g -range (°C)
PS/PPE 100/0	Ha1 ^a	102	96–106
PS/PPE 90/10	Ha3	109	105–114
PS/PPE 75/25	Ha5	122.5	114–129
PS/PPE 60/40	Ha6	134.5	126–143
PS/PPE 50/50	Ha7	144	134–155

^a In order to estimate the degree of degradation caused by this mixing operation, the molecular weight of Ha1 has been determined both from GPC and viscosimetry. A value for M_n of 70 000 and M_w of 170 000 was found, which implies a decrease of the molecular weight of PS by 10% as a result of thermal degradation.

The location of the phase inversion region before and after a quiescent thermal treatment as a function of the viscosity ratio has been compared to some existing model predictions from the literature. A qualitative understanding of the driving forces behind the formation of sometimes complex phase morphologies in the phase inversion region will be given. The impact of the viscosity ratio on droplet break-up processes could be investigated in 1 wt.% blends, and a new model relating the capillary number for droplet break-up with the melt viscosity ratio is proposed.

Finally, the contribution of droplet coalescence to the final blend phase morphology and coarsening rates upon a quiescent thermal treatment will be evaluated as a function of the viscosity ratio.

2. Experimental

2.1. Materials

The characteristics of the basic materials used in this study are listed in Table 1. Polypropylene (PP) is a commercial grade isotactic PP (Elf-Atochem); its melting point is 161°C. Atactic polystyrene (PS) is a commercial grade Styron® E680 supplied by Dow Benelux N.V. Poly (2,6-dimethyl-1,4-phenylene ether) (PPE) is a PPE-800 grade supplied by General Electric.

2.2. Preparation of the miscible amorphous PS/PPE phases

The amorphous phases were prepared by melt-blending PS ($T_g = 102^\circ\text{C}$) with PPE ($T_g = 215^\circ\text{C}$); both components are perfectly miscible over the whole composition range [29,30]. As a consequence it is possible to vary both the melt-viscosity and the glass-transition temperature, T_g , of the amorphous phase without altering the interfacial tension between PP and these miscible amorphous components [31]. Blending has been performed on a Haake Rheocord 90 twin screw extruder after drying the materials overnight at 40°C under vacuum. The mixing conditions were set as follows: screw speed: 120rpm; intake section: 200°C; melting section: 300°C; sections 3 to 5: 285°C; throughput: 10 to 15 g/min. At the die exit, strands were cooled in a water bath and pelletized. The homogeneity of each blend was checked by DSC measurements. Table 2 presents a list of the

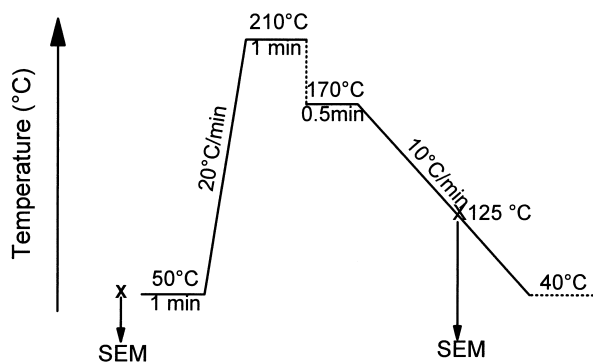


Fig. 1. Thermal program applied to the PP/(PS/PPE) samples, simulating a conventional DSC cooling run.

prepared miscible amorphous phases and the corresponding T_g 's.

2.3. Characterization of the materials

The melt-viscosity of all materials under processing conditions was measured using a high pressure capillary rheometer Rheograph 2002 (Göttfert) with a capillary die of 1 mm and L/D ratio of 30. Measurements were performed at 260°C over a shear rate range, $\dot{\gamma}$, between 10 and 500 s^{-1} . Measurements for a Bagley correction have been performed with capillary dies having an L/D ratio of 20/1 and 10/1. For the shear rate used to calculate the viscosity ratios ($\dot{\gamma} = 50 s^{-1}$), the Rabinowitch correction factor was negligible for the lower viscous materials, i.e. PS, Ha1 and Ha3, and became more important for the more viscous materials; the Bagley correction turned out not to be necessary.

The melt-elasticity of the pure materials has been determined with a RDA-II rheometer (Rheometric Scientific) in plate-plate configuration. Samples with a diameter of 25 mm and a thickness of 2 mm were dried at 80°C under vacuum. Measurements were performed at 260°C under nitrogen atmosphere at a constant strain of 10% from 1 to 100 rad/s. It was assumed that the Cox–Merz rule, $\eta^*(\omega) = \eta(s^{-1})$, is valid.

The interfacial tension, σ_{12} , of the PP/(PS/PPE) blends was determined both via the breaking-thread method and pendant-drop analysis in order to estimate the influence of the PPE concentration in the miscible PS/PPE phase on the value of σ_{12} . The detailed results of these measurements are presented elsewhere [31].

2.4. Compounding of the PP/(PS/PPE) blends

Prior to the melt-blending operations, all materials were dried under vacuum at 50°C overnight. The materials were then melt-blended in a mini-extruder (DSM Research, The Netherlands), which is a conical co-rotating fully intermeshing twin-screw extruder, with a capacity of about 4 cm^3 . A recirculation channel allows varying of the blending time. All blends were prepared under nitrogen atmosphere to prevent oxidative degradation.

Blending conditions were chosen carefully by variation of rotor speed, blending temperature and mixing time. The optimal blending conditions resulting in an equilibrium phase morphology for both low viscous and high viscous materials, were a mixing temperature of 260°C during 10 min at a screw speed of 50 rpm. After blending, the melt was immediately quenched at the die exit in an isopropanol/solid CO_2 mixture.

PP/(PS/PPE) blends were prepared for PP12/Ha1, PP12/Ha3 and PP12/Ha7 over the whole composition range. Blend compositions (in wt.%) were 99/1, 90/10, 80/20, 70/30, 60/40, 50/50, 40/60, 30/70, 20/80, 10/90 and 1/99. Moreover, for the analysis of the critical capillary number as a function of viscosity ratio, 1 wt.% dispersions were prepared under the same conditions for PP12/PS, PP12/Ha5, PP40/Ha5, PP40/Ha6 and PP40/Ha7.

In order to evaluate the rate of phase coarsening as a function of blend composition and viscosity ratio, p , a typical thermal program as commonly used during dynamic crystallization measurements in DSC has been applied to all samples (Fig. 1). Extruded strands were therefore thermally treated in a Mettler hot-stage with FP-90 central processor, and the newly obtained blend morphology was analyzed in the same way as the as-extruded blends.

2.5. Morphological analysis

A Scanning Electron Microscope, SEM, (Phillips XL20), operated at an accelerating voltage of 20kV, was used to examine the size and distribution of the dispersed phase. Fracture surfaces perpendicular to the extrusion direction were obtained by brittle fracture in liquid nitrogen. In the case of samples with a dispersed PS/PPE phase, etching of the minor phase was performed by stirring the samples for 48 h in chloroform at room temperature. In the case PP formed the dispersed phase, etching was impossible, because PP only dissolves at elevated temperatures, causing partial melting of the PS/PPE matrix and morphological changes. All samples were dried and subsequently coated with a conductive gold layer.

An image analysis apparatus (Pericolor 1500) was used to quantify the size of the dispersed phase. For statistical reasons, at least six SEM micrographs spread well over the sample core region were analyzed, each containing on average 100 to 200 dispersed domains. As such, a relevant number-average diameter, D_n , and weight-average diameter, D_w , were obtained together with the particle size distribution in each blend system. Further, the perimeter and planar area of each structure in the micrographs were quantified.

Because SEM micrographs only provide information on the sample morphology perpendicular to the extrusion direction, additional solubility experiments were performed to assess the region of phase inversion. Samples were immersed for two hours in chloroform, a solvent for

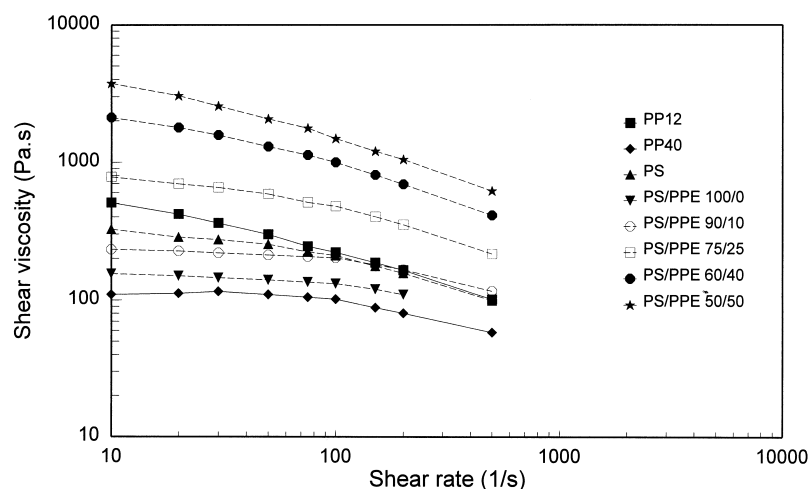


Fig. 2. Melt-viscosity of the materials, measured at 260°C, as a function of shear rate.

PS/PPE. Only in the case the PP phase forms a cocontinuous network structure, the sample will retain its original shape.

3. Results and discussion

3.1. Melt-viscosity and melt-elasticity of the blend components

In order to calculate the viscosity ratio, p , of the blend components for the applied processing conditions, capillary rheometry measurements were performed at the blending temperature of 260°C. Because the melt-mixing in the mini-extruder has been performed at a constant screw speed of 50 rpm, the rheological behaviour of each component is best reflected by its melt-viscosity measured at a constant shear rate. As it is difficult to determine the exact shear rate in the mini-extruder during the blending process, a shear rate of roughly 50 s^{-1} , calculated by the method of Heidemeyer [32] and Wu [8], was used. In general, shear rates for conventional large scale extrusion equipment are situated in the range of $50\text{--}500 \text{ s}^{-1}$ [33]. The melt-viscosity

of all components as a function of shear rate is presented in Fig. 2.

The viscosity ratios were determined at 260°C and 50 s^{-1} (Table 3). By varying the concentration of the PP12 phase, and the amount of PPE in the miscible amorphous PS/PPE phase, it becomes possible to obtain viscosity ratios in the range from 0.14 up to 7. Blends of PP12 with Ha3 (PS/PPE 90/10) approach most closely the condition of equal melt-viscosities ($p \approx 1$).

To allow a more complete interpretation of the results on blend phase morphology development, the melt-elasticity of all components was determined under the same processing conditions (260°C, 50 s^{-1}) with a plate-plate rheometer. The results are listed in Table 4. The melt-elasticity ratios turned out to be comparable to the melt-viscosity ratios listed in Table 3.

3.2. Blend phase morphology of melt-mixed and thermally treated PP12/(PS/PPE) blends

The blend phase morphology of a low viscous/low viscous as-extruded blend series (PP12/Ha1) and a low

Table 3
Viscosity ratio for two different blends, PP12/(PS/PPE) and PP40/(PS/PPE), at 260°C for a shear rate of 50 s^{-1}

PP12/(PS/PPE)			
Material	η (Pa s) (260°C, 50 s^{-1})	PP12 matrix ($\eta = 297 \text{ Pa s}$)	PP12 dispersed ($\eta = 297 \text{ Pa s}$)
PS E680	252	0.85	1.2
Ha1	120	0.5	2.0
Ha3	204	0.7	1.5
Ha5	588	2.0	0.5
Ha7	2068	6.9	0.14
PP40/(PS/PPE)			
Material	η (Pa s) (260°C, 50 s^{-1})	PP40 matrix ($\eta = 110 \text{ Pa s}$)	PP40 dispersed ($\eta = 110 \text{ Pa s}$)
Ha5	588	5.4	0.19
Ha6	1303	11.8	0.08
Ha7	2068	18.8	0.05

Table 4
Melt-elasticity and elasticity ratio of the raw materials at 260°C for a shear rate of 50 s⁻¹

Material	G' (Pa) (260°C, 50 s ⁻¹)	Melt-elast. (Pa s)	%Elastic	Elast. ratio PP12 matrix	Elast. Ratio PP12 dispersed
PP12	6981	140	47	—	—
PP40	1431	29	26	—	—
PS E680	3889	78	12	0.56	1.79
PS/PPE 100/0	2215	44	37	0.32	3.1
PS/PPE 90/10	4141	83	41	0.59	1.69
PS/PPE 75/25	10 198	204	35	1.46	0.68
PS/PPE 50/50	38 316	766	37	5.49	0.18

viscous/high viscous as-extruded blend series (PP12/Ha7), and their corresponding thermally treated blends is represented in Fig. 3(a) and (b) respectively. The blend phase morphology of PP12/Ha3 blends is not displayed, but behaves quite similar to that observed in the PP12/Ha1 blends.

It is clearly illustrated that a change in the *viscosity ratio* for the same blend composition has a significant effect on the blend phase morphology and on the phase inversion region. A detailed discussion on this topic is presented in the next section.

Further, blends of PP12 with Ha7 (PS/PPE 50/50) show a complex *composite-like* phase morphology, which becomes even more pronounced after a thermal treatment of the blends. Even at the low concentration of 20 wt.% PP12, the highly viscous PS/PPE 50/50 phase forms a dispersed-like phase of large domains which contain a considerable amount of PP12 subinclusions. This peculiar phase morphology can be observed over a broad composition range, from 20 wt.% PP till even 60 wt.% PP in the as-extruded blends. The formation of a similar composite-like blend morphology has been reported for PP/PC blends near the phase inversion region (50/50 vol.%) by Favis et al. [34]. This type of phase structure is similar to some rubber-modified thermoplastics such as high impact polystyrene (HIPS), although the mode of preparation is completely different. Berger et al. [35] assumed that the formation of subinclusions in PET/PA-6 blends was related to an elasticity difference between both phases. In one particular case, a high viscosity ratio was assigned as the cause for the formation of a composite-like morphology.

In the case of PP/Ha7 blends, subinclusion formation occurs only as long as the PP phase forms the continuous and/or cocontinuous phase. Hence, it is rather unlikely that the formation of a composite-like phase morphology must be understood on the basis of differences in melt-elasticity. It seems that the phase inversion in these blend systems is most likely retarded by the presence of the highly viscous (slowly softening) PS/PPE 50/50 (Ha7) phase. Partial phase inversion is gradually proceeding until the viscous Ha7 phase becomes the matrix. During melt-mixing, the low viscous PP phase acts as a lubricant to minimize the energy of mixing, and hence retards the liquefaction process of the higher softening PS/PPE 50/50 [36]. Similar results have

been found by Sundararaj et al. [37,38]. These authors assigned this phenomenon to a difference in softening temperature of both components. The lower melting component will always first encapsulate the higher melting component to form the matrix phase; only if a substantial amount of the higher melting component has softened, gradual phase inversion can proceed, causing this complex composite-like phase morphology.

3.3. Region of phase inversion

As can be observed from Fig. 3, a change in the viscosity ratio has a pronounced effect on the location of the region of phase inversion. Blending a highly viscous and low viscous material, as in PP12/Ha7 blends, causes the region of co-continuity to shift towards lower contents of the low viscous phase. Similar observations have been reported by Favis and Chalifoux [20] and Elemans [39].

Jordhamo et al. [40] developed an empirical model based on the melt-viscosity ratio, η_d/η_m , and the volume fractions, ϕ , of each phase for predicting the phase inversion region in immiscible polymer blends. According to this model, phase inversion should occur when the following equation holds:

$$\frac{\eta_1 \phi_2}{\eta_2 \phi_1} = 1. \quad (5)$$

Jordhamo's model however is limited to low shear rates, and does not take into account the effect of variations in the interfacial tension between the phases. From the experimental results, shown in Fig. 4, it is clear that although all blends were prepared at relative low shear rate conditions (50 s⁻¹) and at comparable values of the interfacial tension, Eq. (5) does not always predict the region of phase inversion correctly, especially when blending materials with a large difference in melt-viscosity. A similar observation has been reported by Chen and Su [41]; these authors ascribed this discrepancy to the fact that Eq. (5) overestimates the volume fraction of the high viscosity phase, and proposed an alternative equation (Eq. 6)

$$\frac{\phi_{hv}}{\phi_{lv}} = 1.2 \left(\frac{\eta_{hv}}{\eta_{lv}} \right)^{0.3} \quad (6)$$

where the subscripts "hv" and "lv" denote the high and the low viscosity phase, respectively.

Chen and Su [41] explained the asymmetric equation as a result of post-mixing coarsening, which depends more heavily on the matrix viscosity, and this effect will be more pronounced at compositions rich in the low viscous phase. A comparison of the experimental results of PP12/(PS/PPE) blends with Eq. (6) shows a quite good correlation, even for blends of components with extreme differences in melt-viscosity, as in PP/Ha7 blends. An even better description of the region of phase inversion in PP12/(PS/PPE) blends is given when removing the factor 1.2 from Eq. (6), as shown in Fig. 4.

It is however remarkable that a *quiescent thermal treatment* does not really seem to alter the *location* of the region of phase inversion significantly. In the experimental results presented in this article, a thermal treatment after mixing caused mainly a pronounced phase coarsening of the co-continuous structures in the low viscous blends, with only a slight shift of the phase inversion region towards higher concentrations of the PP phase in the blend. For the blends in which a highly viscous phase (Ha7) was mixed with the much lower viscous PP12 phase, the thermal treatment was not long enough to really influence the quite immobile, highly viscous blend phase morphology and provoke a phase inversion.

A more surprising result of the thermal treatment on the *phase morphology* in the region of phase inversion was observed for the low viscous PP/Ha1 and PP/Ha3 blends (Fig. 5). A thermal treatment not only causes the co-continuous structures to coarsen with at least a factor 5, it also induces the formation of a composite-like equilibrium phase morphology, in which both phases contain subinclusions of the other phase. As such, a completely different phase morphology, which can affect the blend properties, is formed. It is not really clear yet what are the driving forces behind this mechanism. Both blend systems consist of two phases with a nearly equal melt-viscosity and melt-elasticity. The hypothesis formulated by Berger et al. [35], that composite-like morphologies would be formed as a result of elasticity differences between both phases, does not agree with our experimental findings. Quintens et al. [42] demonstrated that post-mixing coarsening can result in changes from a dual-phase continuity to a typical droplet-in-matrix morphology and vice-versa, depending on the blend composition. Hence, it can be understood that a dynamic equilibrium in the phase inversion region during the coarsening process is responsible for the observed composite-like phase morphology in thermally treated low viscous/low viscous blend systems.

The phase morphology in the region of phase inversion in a low viscous/high viscous blend system, as in PP/Ha7, did neither show strong phase coarsening, nor a change in the type of composite-like structures.

3.4. Influence of the blend composition on the phase morphology of as-extruded PP/(PS/PPE) blends

Fig. 6(a) shows the evolution of the weight average

particle diameter in PP12/(PS/PPE) blends as a function of blend composition for the three main blend series under investigation. The corresponding width of the particle size distribution curve is presented in Fig. 6(b).

As expected, most blends show an increase in the average particle diameter, along with a broadening of the particle diameter distribution, as the amount of dispersed phase increases. This is typically related to droplet coalescence during melt-mixing, which is known to be a random process, hence broadening the particle size distribution. Several authors have observed a similar behaviour previously [20,21,43]. It has to be noticed that, depending on the viscosity ratio of the components during melt-mixing, the amount of coalescence differs. Moreover, for the same blend system, an asymmetric influence of phase coarsening is observed. Because the interfacial tension in all blends is nearly the same, it is possible to evaluate solely the influence of the viscosity ratio on droplet break-up and coalescence rate. This will be discussed in more detail in the following two sections.

In the case of low viscous PP/Ha1 and PP/Ha3 blends, the influence of the viscosity ratio on the degree of phase coarsening during melt-mixing at higher blend compositions, can be qualitatively explained based on coalescence theories [4,5,11]. In blends with a dispersed PP phase (variable η_m), a lower viscosity ratio results in a less pronounced phase coarsening, especially for higher contents of the PP phase. This can be understood from the fact that if the matrix phase is more viscous, both higher flow forces and hence decreasing collision times, along with a more difficult matrix inter-layer film drainage between the colliding droplets, reduce the coalescence probability. In blends with PP as the matrix phase ($\eta_m = \text{cte}$), the influence of the viscosity ratio on the degree of coalescence during melt-mixing is less pronounced. The slightly higher coalescence observed in blends with a lower viscosity ratio (lower η_d) is more complex to interpret.

It should be mentioned that the phase morphology of blends of a lower viscous PP with the highly viscous Ha7 behaves somewhat different. First of all, subinclusions of the continuous PP phase within the dispersed Ha7 domains tend to be only the result of a droplet break-up process, as their average sizes and size distributions are independent of blend composition and comparable with the particle size found in PP/Ha7 1/99 blends. As it can be assumed that coalescence phenomena in 1wt.% blends are generally negligible, the latter is a good measure for the minimum obtainable droplet diameter in a blend system during melt-mixing. This would indicate that the composite-like morphology is typically formed in slowly developing phase morphologies. The formed subinclusions are subsequently immobilized by the surrounding highly viscous domains and coalescence becomes rather difficult [37,38].

Another remarkable observation is that the minimum obtainable droplet diameter, as observed in blends containing only 1 wt.% of the dispersed phase, in blends with Ha7

**PP/(PS/PPE)
Blends
As-extruded**

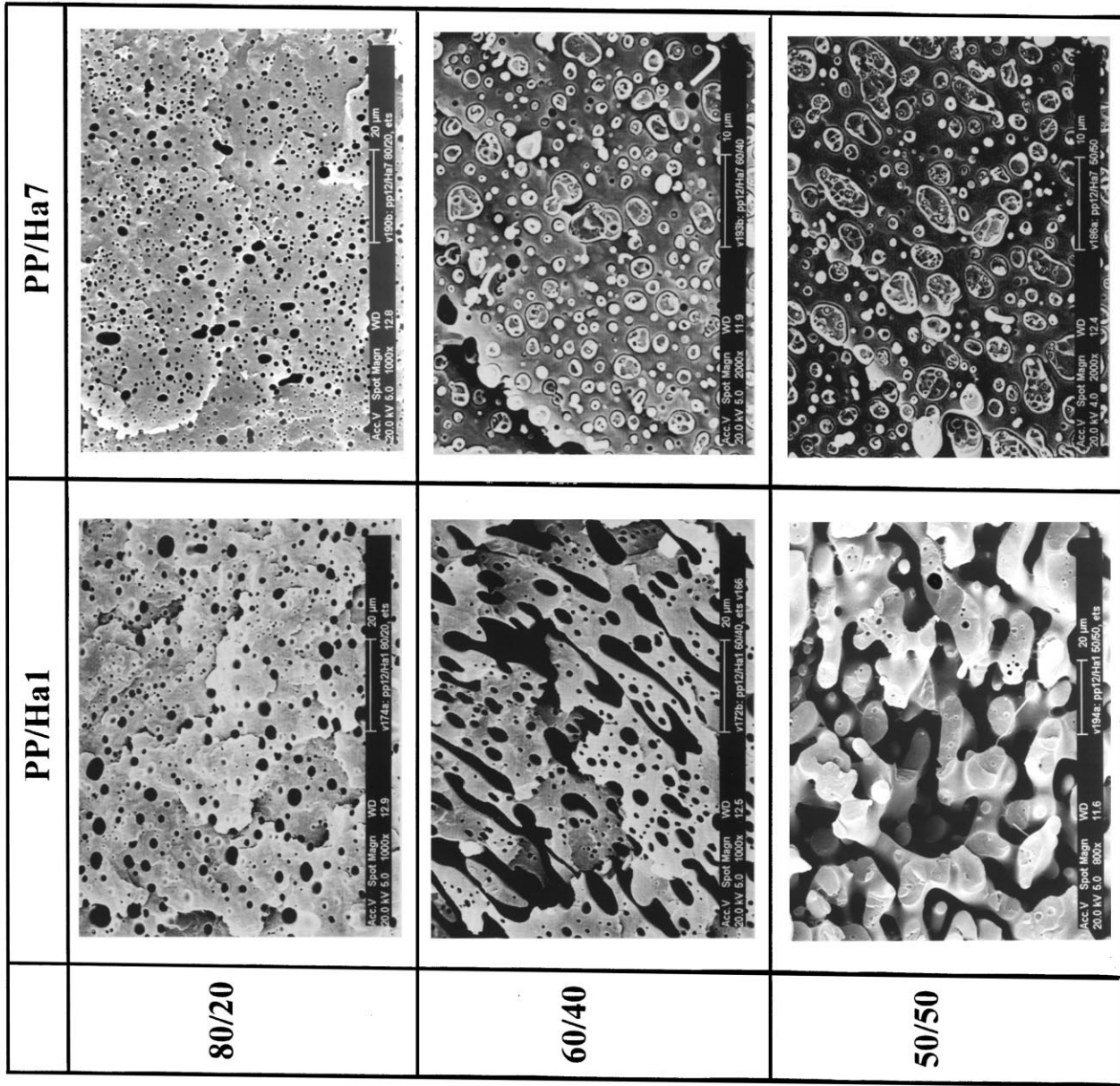


Fig. 3. Blend phase morphology of some selected PP12/(PS/PPE) blends (a) after melt-mixing and quenched at the die exit; (b) after a quiescent thermal treatment simulating a conventional DSC cooling run. Note the difference in magnification for the several micrographs.

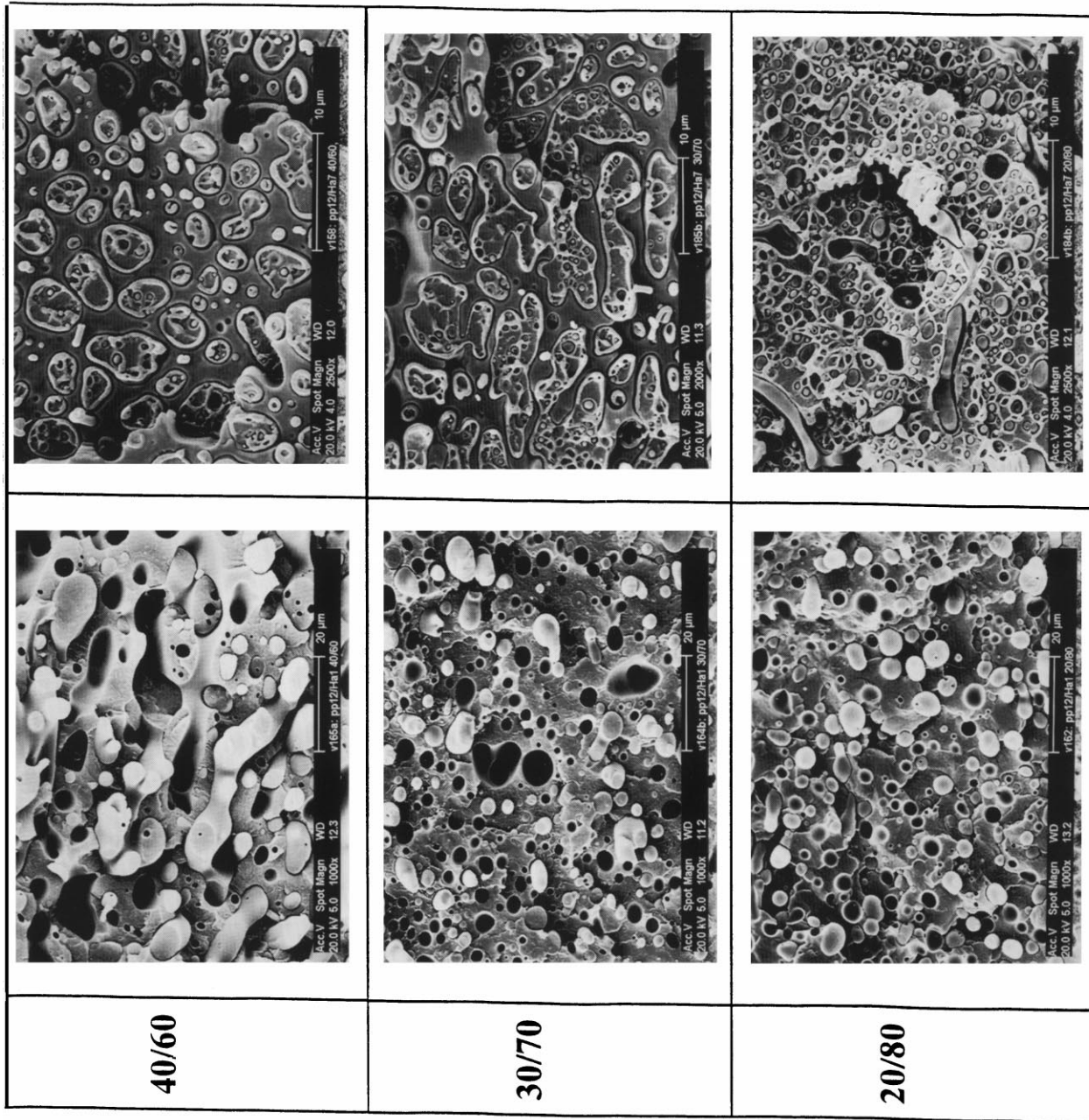


Fig. 3. (continued)

**PP/(PS/PPE)
Blends
DSC-treated**

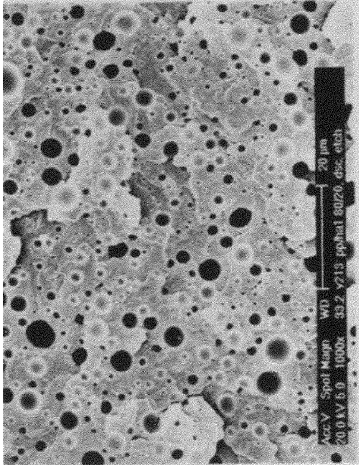
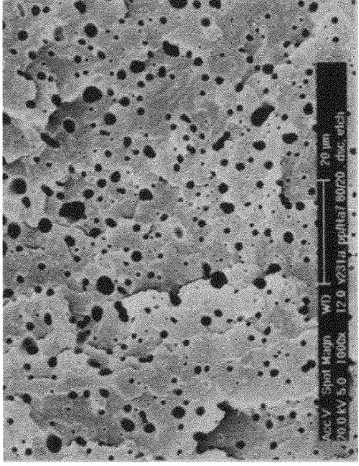
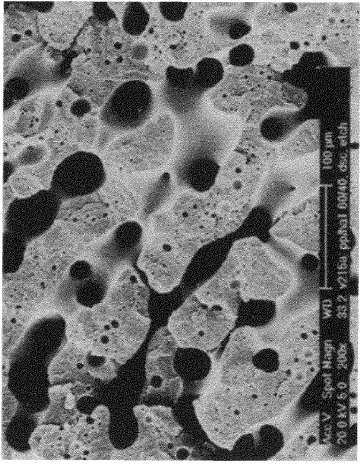
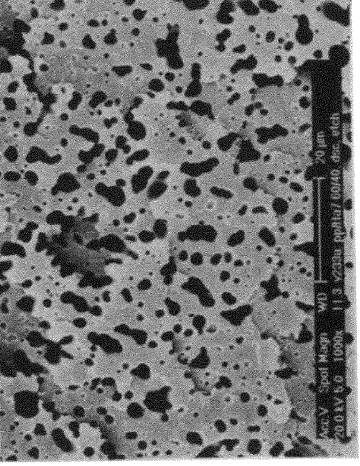
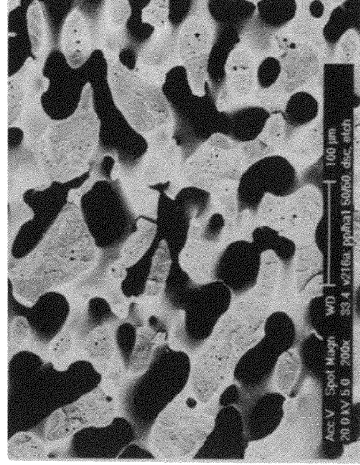
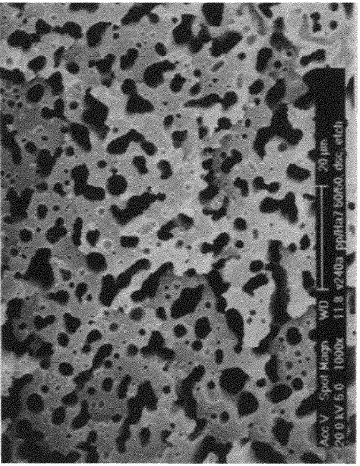
	PP/Ha1	PP/Ha7
80/20		
60/40		
50/50		

Fig. 3. (continued)

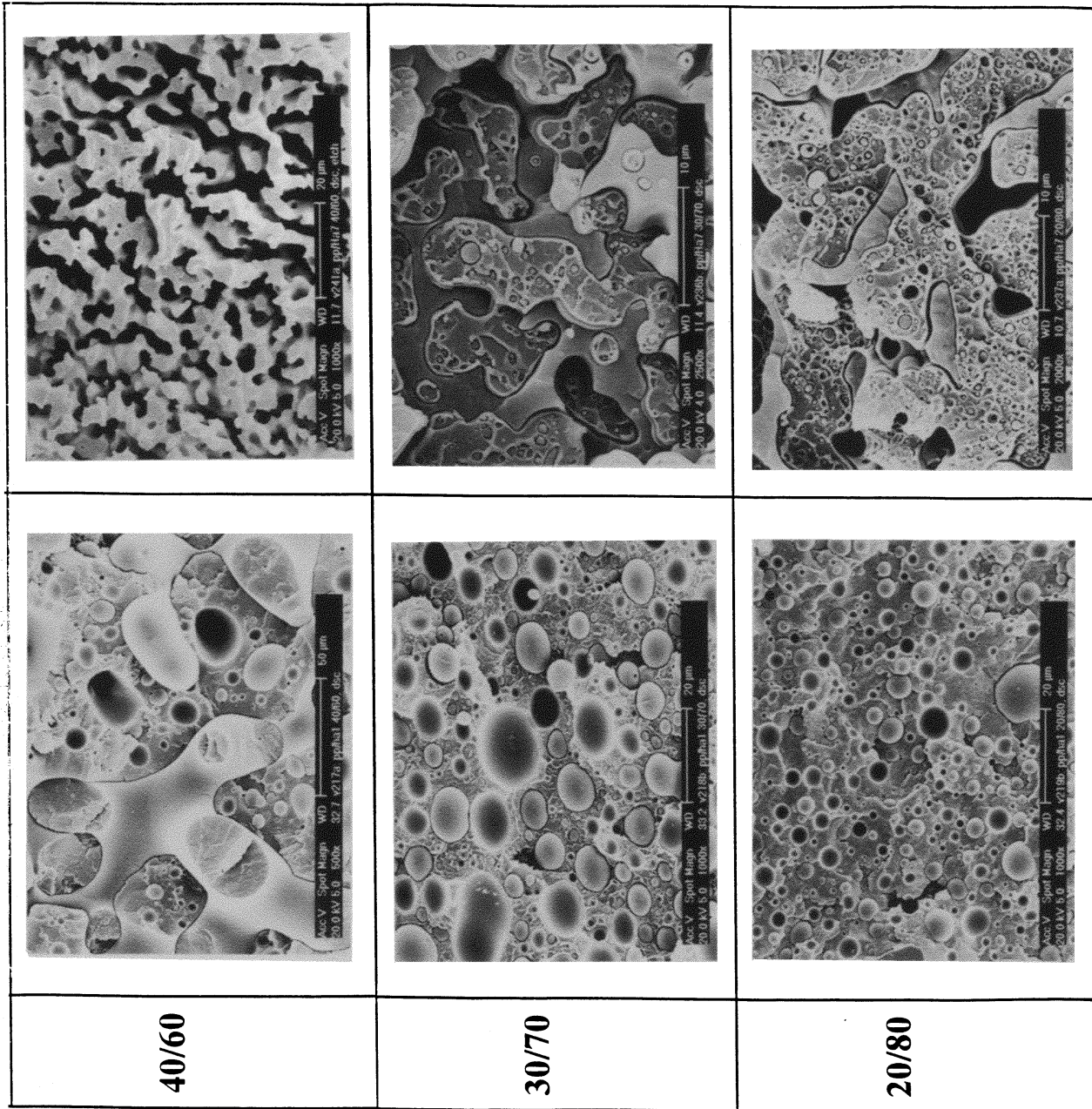


Fig. 3. (continued)

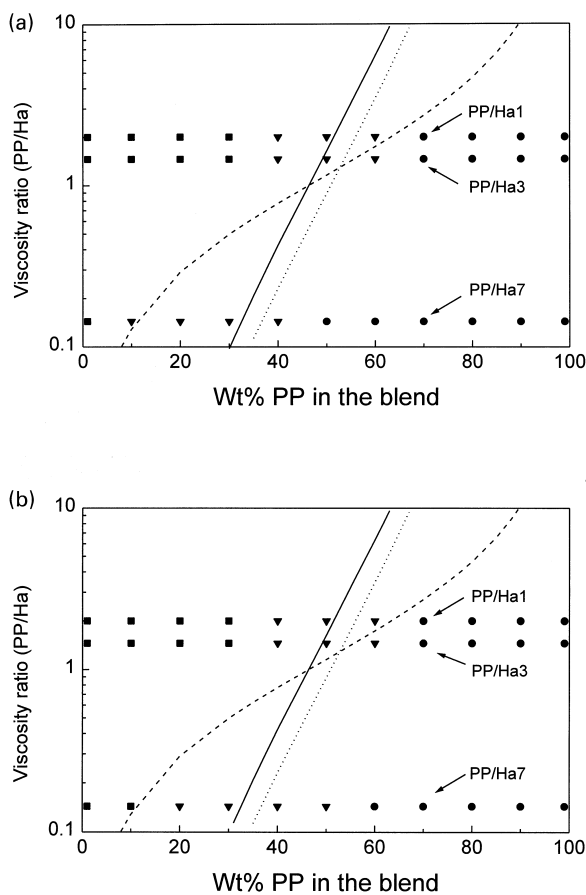


Fig. 4. Influence of the melt-viscosity ratio, p , on the phase inversion region in PP12/(PS/PPE) blends for (a) as-extruded blends and (b) after a quiescent thermal treatment simulating a conventional DSC run. Blends where PP is the dispersed phase (■), with a cocontinuous phase morphology (▼), and where PP is the continuous matrix phase (●). The region of phase inversion is fitted according to Eq. (5) of Jordhamo et al. (dashed line), Eq. (6) of Chen and Su (dotted line), and the modified Eq. (6) without factor 1.2 (full line).

dispersed in a lower viscous PP matrix, seems to be much higher than the particle diameter observed in PP/Ha7 blends with a higher content of the dispersed phase. This tendency does not obey any existing theory on coalescence. No satisfying explanation for this phenomenon could be found in literature. This behaviour seems to be observed typically in immiscible polymer blends having a low viscous matrix in which minor amounts of an extremely high viscous phase, e.g. PS/PPE 50/50 (Ha7), has to be dispersed. A similar result has been found in blends of a low viscous PA-6 matrix ($M_w = 18\,000$) with a highly viscous SAN/SMA 96/4 dispersed phase [44].

A first hypothesis is that the size of the dispersed phase, as measured on fracture surfaces perpendicular to the extrusion direction, decreases with increasing amount of the highly viscous and highly elastic Ha7 phase, as a consequence of the formation of slender fibrils instead of the normal droplet-in-matrix phase structure. Berger et al. [45], Lyngaae-Jørgensen et al. [46], and Favis and Therrien

[21] have observed preferential fibril formation for a more elastic dispersed phase at higher viscosity ratios. The latter authors [21] ascribed this to the sensitivity of the morphology of the minor phase to die-effects. More recently, new investigations on PC/PP blends confirmed indeed that the size of a highly viscous dispersed phase in a low viscous matrix is much smaller than that of the complementary blend [47]. This was ascribed to the fact that deformation in an elongational flow field is not sensitive to the viscosity ratio, as calculated with values of melt-viscosity obtained in shear flow. Because in the mini-extruder used for the preparation of the immiscible PP12/(PS/PPE) blends, the time of mixing can be varied by recirculating the melt from the end of the screws back to the feeding zone by a quite narrow recirculation channel, elongational flow could have played a role in the development of the phase morphology. Careful examination of the SEM micrographs of these PP/Ha7 blends however shows a clear droplet-like phase morphology. Hence, there must be another reason for the observed behaviour.

Another explanation that can fit these results is based on the different amount of total mixing energy supplied to the blend system during its preparation. All blends were prepared under the same processing conditions, i.e. not only a constant mixing temperature and time, but also a constant mixing speed of 50 rpm (or shear rate of about 50 s^{-1}). In the case both phases have nearly equal melt-viscosities, as in PP/Ha1 and PP/Ha3 blends, the total energy input remains fairly constant. Also in the case where the matrix viscosity is much higher than the dispersed phase viscosity, the addition of minor amounts of a low viscous component will not significantly alter the total energy input in the blend systems, hence allowing the dispersed phase to undergo normal coalescence. In the peculiar case when a highly viscous, slowly softening, Ha7 phase is added to a low viscous PP matrix, the blend viscosity is expected to suddenly increase by the presence of these relatively rigid droplets; a higher energy input is thus required to attain the preset requirement of 50 rpm during melt-mixing. It is expected that this will cause higher dispersive forces, along with a lower coalescence probability (shorter collision times). Hence, upon addition of higher amounts of a highly viscous component (Ha7), a finer phase morphology will be formed.

3.5. Influence of the viscosity ratio on the droplet break-up process in PP/(PS/PPE) blends-comparison with existing theories

The influence of the viscosity ratio, p , on droplet break-up can be evaluated from the curve obtained for 1 wt.% dispersions, for which it can be assumed that coalescence is fairly negligible. Besides the experimental data available from the blends prepared for the main part of this research, some additional 1 wt.% blends containing a lower molecular weight polypropylene (PP40) were prepared to evaluate a

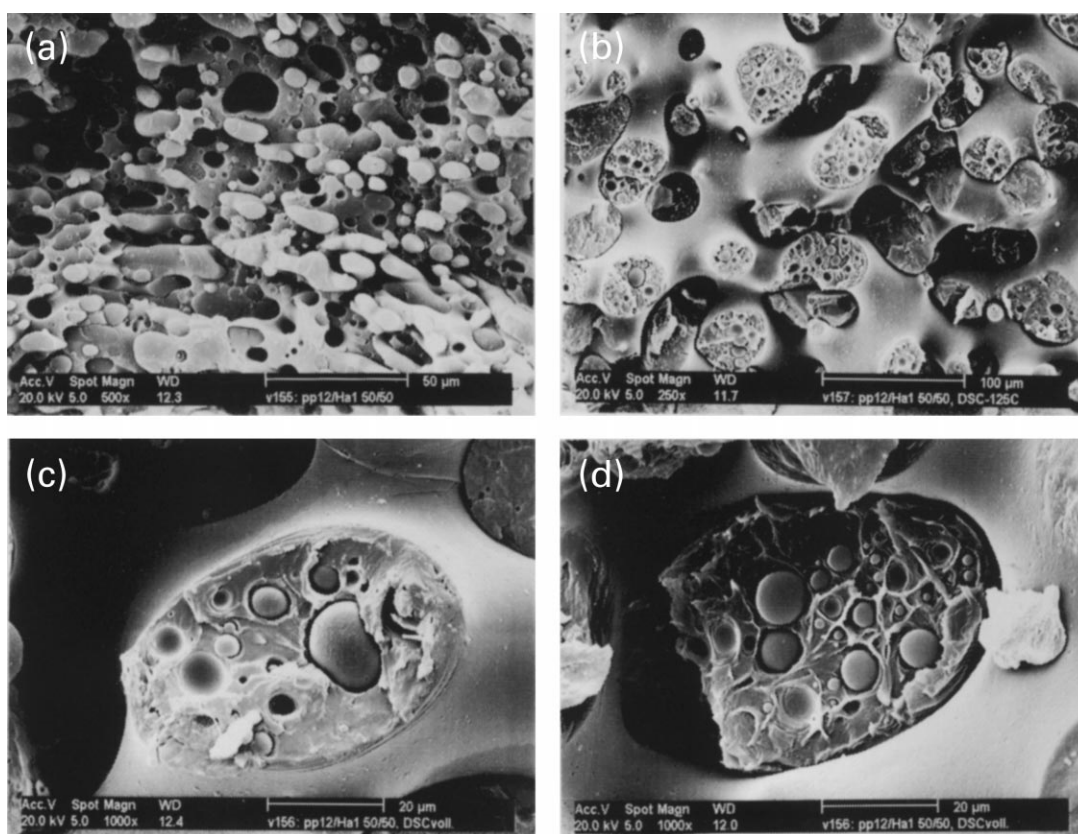


Fig. 5. Influence of a quiescent thermal treatment simulating a conventional DSC run, on the blend phase morphology in the phase inversion region for a PP12/ Hal 50/50 blend. Note the difference in magnification of the displayed micrographs. (a) as-extruded blend, global overview; (b) DSC-treated blend, global overview; (c) composite-like phase morphology of PP subinclusions in the co-continuous Hal phase; (d) composite-like morphology of Hal subinclusions in the co-continuous PP phase.

broader viscosity ratio range. As such, the evaluation of the influence of the viscosity ratio could be extended to a viscosity ratio range from 0.05 to 20. The results are presented in Fig. 7.

It is clear that the viscosity ratio plays a crucial role in the droplet break-up process; higher viscosity ratios hamper the droplet break-up process. In this case, the flow field of the low viscous matrix is not able to sufficiently transfer the applied shear stresses to the highly viscous dispersed phase. Additionally, the standard deviation also increases with increasing particle size; this can indicate both a retarded break-up process, or a facilitated coalescence as a consequence of the high mobility of dispersed domains in a low viscous matrix along with a higher coalescence probability [48].

Contrary to what is often claimed and accepted in the literature, at a viscosity ratio of 1.0 the minimum obtainable particle diameter does not show a minimum [8]. A similar observation has been reported by Favis and Chalifoux [19] for melt-mixed PP/PC blends, in which a low concentration (7wt.%) of a low viscous PP phase was dispersed in a more viscous PC matrix. It is important to note that even at a viscosity ratio of 18.8, significant particle disruption has occurred unlike Newtonian systems in a shear flow field

which do not show break-up above $p = 4$. Several authors already reported similar observations for viscoelastic systems at high viscosity ratios [8,19,47]; this can be ascribed to the existence of elongational stresses in the twin-screw mini-extruder, which have been shown to be much more effective in droplet break-up [6,7].

The experimentally observed average particle diameters were compared with the existing theories of droplet break-up. The Taylor-diameter was calculated using Eq. (2), and the number average particle diameter, as predicted by Wu, was calculated according to Eq. (3). For the interfacial tension in PP12/(PS/PPE) and PP40/(PS/PPE), values of 5.5 mN/m and 4.5 mN/m respectively, have been used. These values were determined experimentally both from the breaking-thread method and pendant drop analysis method; more details can be found elsewhere [31]. For all points, the calculations were performed on the basis of the real situation, i.e. a variable matrix viscosity depending on the blend system under investigation. Because the values used for η_m were those experimentally determined via capillary rheometry, some scatter can be observed in the calculated values for the Taylor- and Wu-diameter. However, the tendencies of both predictions as a function of viscosity ratio are obvious. The experimentally observed data are

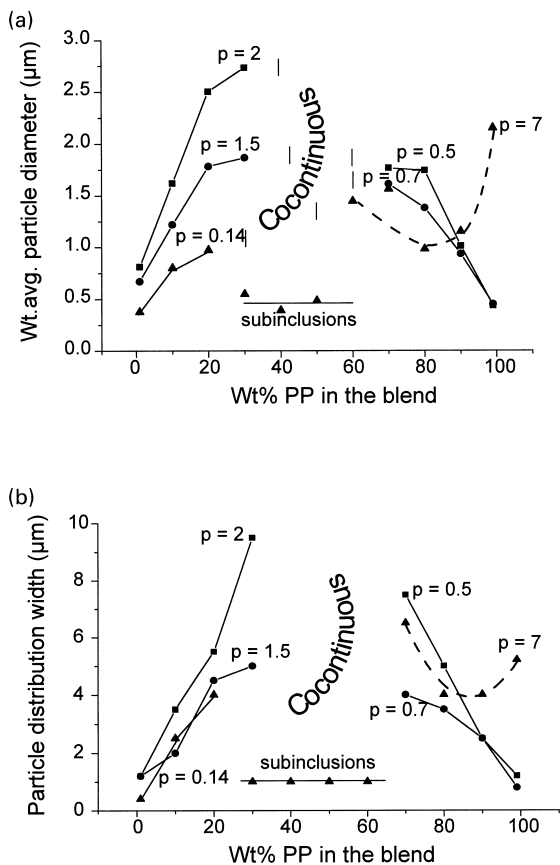


Fig. 6. Evolution of (a) the weight-average particle size; and (b) the total width of the particle size distribution in as-extruded melt-mixed PP12/(PS/PPE) blends. (■) PP/Hal blends; (●) PP/Ha3 blends; (▲) PP/Ha7 blends.

found to be located in between the theoretically minimum obtainable particle diameter as predicted by Taylor (Eq. 2) and the empirically particle diameter as proposed by Wu (Eq. (3)).

For low viscosity ratios ($p < 0.5$), the experimentally observed particle diameters agree fairly well with the

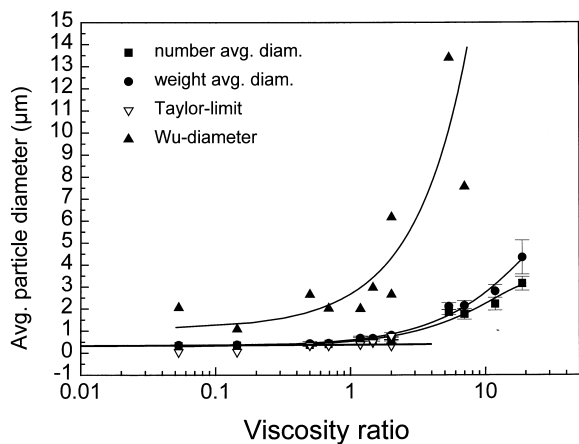


Fig. 7. Influence of the viscosity ratio, p , on the droplet break-up process in PP/(PS/PPE) blends (both PP12 and PP40) with 1 wt.% dispersed phase.

extrapolated values for the Taylor diameter. In this region, changes in the viscosity ratio do not have a pronounced effect on droplet break-up processes; this observation agrees with the findings of Grace [7]. At low viscosity ratios, shear stresses are very effectively transferred by the highly viscous matrix, and the obtained droplets are the result of an equilibrium between shear forces and interfacial forces only, as accepted for Newtonian systems.

For blend systems with a high viscosity ratio ($p \geq 2$), the prediction of Taylor clearly underestimates the experimentally observed particle diameters. In such blend systems, the low viscous matrix is not very efficient in transferring shear stresses to the highly viscous dispersed domains, and acts more as a lubricating film around these domains.

The empirical equation proposed by Wu (Eq. (3)) results in an overestimation of the average particle diameter over the whole viscosity ratio range. However, this equation was deduced from experimental data on blends containing 15 wt.% of the dispersed phase. Assuming that this equation form still remains applicable, our experimental data could be fitted fairly well according to the following equation

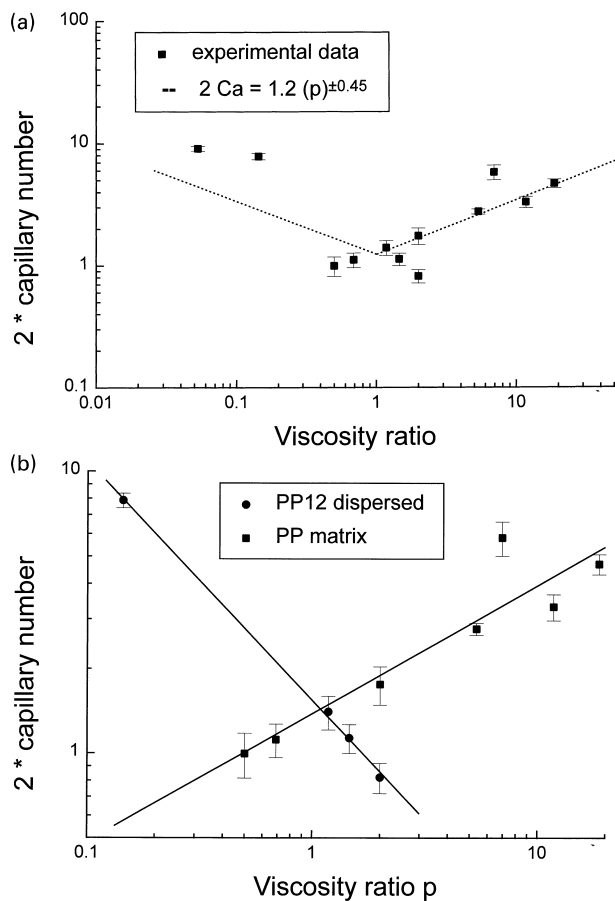


Fig. 8. Influence of the viscosity ratio on the critical capillary number, $(Ca)_{crit}$, for droplet break-up in PP12/(PS/PPE) and PP40/(PS/PPE) blends. (a) Global fitting of the experimental data according to Eq. (7); (b) selective fitting of the experimental data for blends with PP as the dispersed phase and blends with PP as the matrix phase separately.

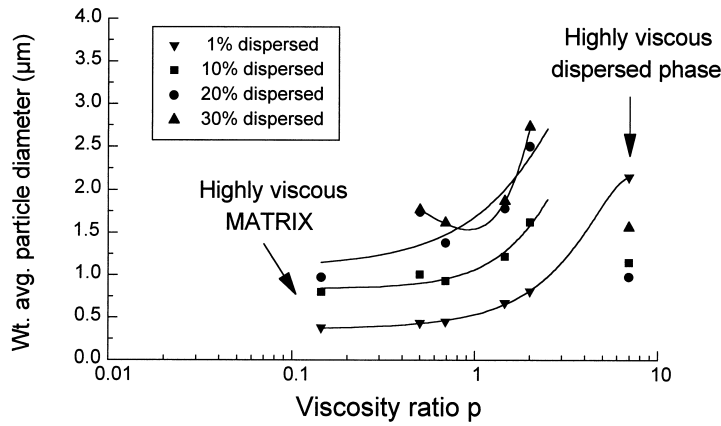


Fig. 9. Influence of the melt-viscosity ratio, p , on the average diameter in as-extruded PP12/(PS/PPE) blends.

(Eq. 7). The results of this fitting is graphically represented in Fig. 8(a),

$$2Ca = \frac{\eta_m \dot{\gamma} D_n}{\sigma_{12}} = 1.2 \left(\frac{\eta_d}{\eta_m} \right)^{\pm 0.45} \quad (7)$$

where the sign of the exponent is positive for $p > 1$ and negative if $p < 1$. It is interesting to note that the factor 4, proposed by Wu, can be removed from Eq. (3) with much better fitting results; at low viscosity ratios, a better fitting of the experimental data and a quite good correlation with the

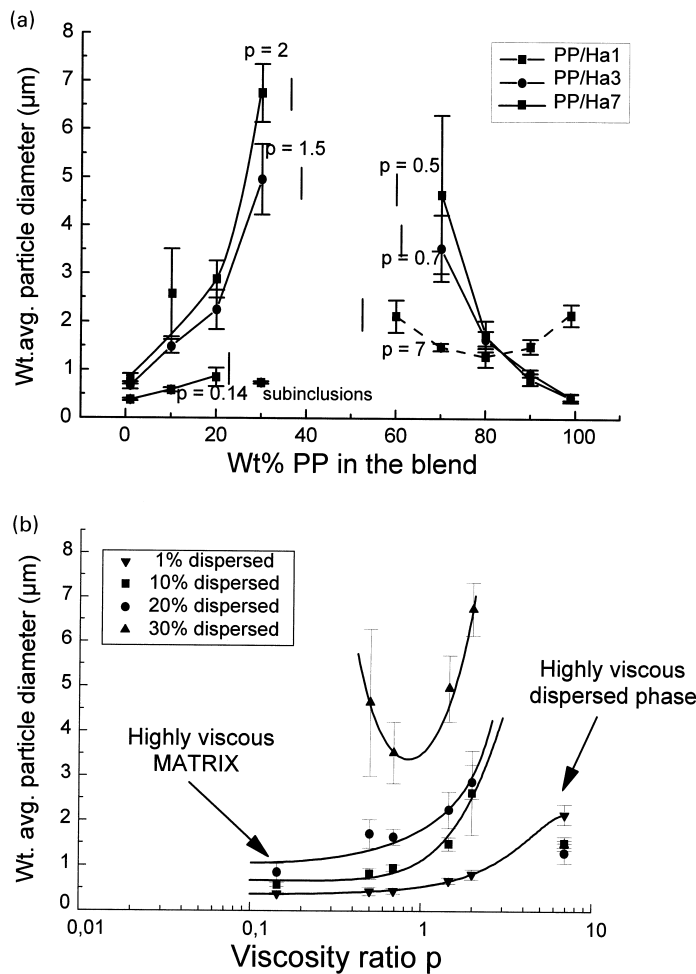


Fig. 10. Influence of (a) the blend composition and (b) the melt-viscosity ratio, on the average particle diameter in PP12/(PS/PPE) blends, after a quiescent thermal treatment simulating a conventional DSC run.

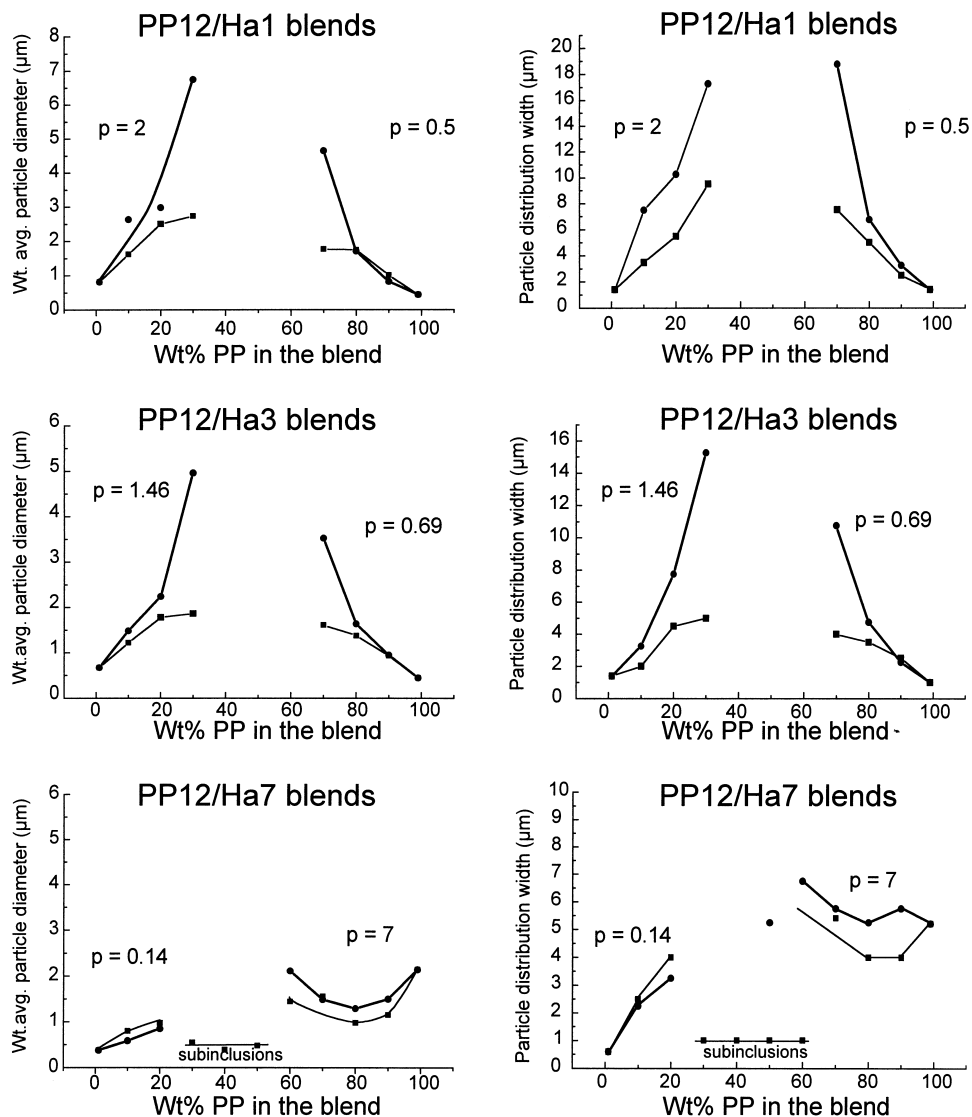


Fig. 11. Influence of a quiescent thermal treatment on the particle size of the dispersed phase in PP12/(PS/PPE) blends. As-extruded blends (■) and thermally treated blends (●).

Taylor diameter were found. The value of the exponent, which decreases from 0.84 to 0.45, is probably very characteristic for each equipment used and reflects possibly the amount of shear versus elongational forces active in the twin-screw mini-extruder.

It should be mentioned that the critical capillary number for droplet break-up still tends to show a minimum at a viscosity ratio around 1. However, it has been demonstrated in Fig. 7, that a minimum in the critical capillary number is not directly related to the smallest obtainable droplet diameter in the case of a varying matrix viscosity.

It was observed that, especially in the viscosity ratio range around 1, different values for Ca_{crit} were found, depending on whether the PP phase formed the matrix or the dispersed phase. A separate fitting of our experimental data points seemed to be much more consistent (Fig. 8(b)), although both curves still show a cross-over point at a

viscosity ratio of 1. This can indicate that the estimation of Ca_{crit} from Eq. (7) remains predominantly valid, but should be further refined somewhat. This observation can be supported by the experimental results published by Oshinski et al. [49] on the phase morphology in a 20/80 wt.% blend of SEBS-g-MA with PA-6. All blends were prepared under identical conditions, as was done in this work. The authors found a strong dependence of the dispersed phase droplet diameter on the melt-viscosity ratio, but no minimum could be observed at a viscosity ratio of unity, as suggested by Wu [8], even for the non-maleated rubbers.

3.6. Influence of the viscosity ratio on the phase morphology of as-extruded PP/(PS/PPE) blends

The evolution of the weight average particle diameter of

the dispersed phase in PP12/(PS/PPE) blends as a function of the viscosity ratio is represented in Fig. 9.

The influence of the viscosity ratio is obvious, both on the droplet break-up process and on the coalescence rate. Again it should be noticed that equal melt-viscosities do not always guarantee a fine phase morphology. Blends containing only up to 20 wt.% of the dispersed phase show a finer blend phase morphology with decreasing viscosity ratio. This can be attributed to the fact that for lower concentrations of the dispersed phase, the droplet break-up process still dominates over coalescence. Hence, it becomes clear that blends with a low viscosity ratio and not too high concentrations of the dispersed phase offer the unique possibility to generate a very fine blend phase morphology, owing to the combination of an enhanced droplet break-up and a somewhat reduced coalescence during melt-mixing. This reduced coalescence probability is directly related to the increase of the matrix viscosity at low viscosity ratios, leading to higher collision forces and hence shorter collision times, more difficult matrix drainage, and highly deformed droplets requiring more interlayer film drainage.

The situation changes when higher amounts of a phase (i.e. > 20 wt.%) are dispersed in the blend system. Droplet break-up becomes now dominated by coalescence processes. The optimal conditions to obtain the finest phase morphology are now observed at a viscosity ratio of unity. A similar behaviour has been reported by Favis and Chalifoux [19] for melt-mixed PP/PC blends with 23 wt.% dispersion. However, these authors found a minimum in the particle diameter at a viscosity ratio of $p \approx 0.15$, which is lower than for our experimental results.

The different behaviour of the phase morphology of blends in which a highly viscous phase is dispersed in a low viscous matrix material is attributed to the change in total mixing energy input as a consequence of a higher blend viscosity, as has been discussed previously.

3.7. Coarsening of the phase morphology of PP12/(PS/PPE) blends upon a thermal treatment

The influence of a thermal treatment (Fig. 1) on the blend phase morphology can be clearly seen from Fig. 3(a) and (b). It can be observed that even a quiescent thermal treatment can result in considerable blend phase coarsening, especially in blends with high concentrations of the dispersed phase and/or lower viscous matrices, and in the region of phase inversion. Growth in the size of droplets dispersed in a matrix was already reported for molten polymer blends kept at a constant temperature at rest [16,50,51].

The result of a thermal treatment on the phase morphology of PP12/(PS/PPE) blends, both as a function of viscosity ratio and blend composition, is presented in Fig. 10(a) and (b), respectively.

Compared to Figs. 9 and 6(a) (as-extruded blends), the most important changes have occurred clearly in blends with a high concentration of the dispersed phase, and/or

blends with nearly equal melt-viscosities. A more direct comparison of the blend phase morphology in PP12/(PS/PPE) blends before and after a quiescent thermal treatment is presented in Fig. 11.

It can be observed that coarsening is most pronounced for blends containing higher concentrations of the minor phase and/or blends having a viscosity ratio close to 1. Only blends with a very highly viscous component, either being the dispersed phase or the matrix phase, do not follow the general tendency. In the case where the highly viscous Ha7 phase is the matrix ($p \ll 1$), this can be ascribed to the low mobility of the dispersed droplets, the shorter collision times, and to their high deformability on collision causing a large area of matrix film to be removed during interlayer drainage [48,52]. This type of blends hence offers the best alternative towards a fine *and* extremely slowly coarsening phase morphology.

From our experimental observations, it becomes clear that equal melt-viscosities do not guarantee a fine phase morphology, as often accepted in literature, nor are they stable when subjected to a thermal treatment. This is especially the case for blends containing higher concentrations of the minor phase.

4. Conclusions

Blending of PP with miscible PS/PPE mixtures offers a model system with the unique opportunity to evaluate the influence of the viscosity ratio on the final blend phase morphology, without affecting the interfacial tension in the blends. The region of phase inversion was found to be shifted with changing viscosity ratios in a way depending more heavily on the matrix viscosity. The formation of composite-like morphologies in this range is observed essentially in PP/(PS/PPE 50/50) blends, and was attributed to the large difference in softening point (and melt-viscosity) of the phases, leading to a slowly developing phase morphology [37,38].

An evaluation of the dependence of the droplet break-up process on the viscosity ratio was performed with blends containing only 1 wt.% of the dispersed phase, in a viscosity ratio range varying from 0.05 to 20. The results show a clear dependence on the viscosity ratio. Highly viscous matrices ($p \ll 1$) enhance droplet break-up owing to their efficient shear stress transfer towards the dispersed phase [23], while low viscous matrices ($p \gg 1$) often act as a lubricant for the dispersed phase reducing the droplet break-up [36]. Comparison of the experimental results with the classical equations proposed by Taylor [6] and Wu [8] reveal that the Taylor limit agrees well with the experimental data at low viscosity ratios ($p < 1$). A modified relationship between the viscosity ratio and the critical capillary number, based on the model proposed by Wu (Eq. (3)), could fit our experimental results quite reasonably. A minimum value for Ca_{crit} was observed around a viscosity ratio of 1. It was however

clearly illustrated that a minimum in Ca_{crit} is not directly related to a minimum in the droplet size, in the case of a varying matrix viscosity.

The influence of the viscosity ratio on droplet break-up is reflected in the particle diameter in blends with a concentration of the dispersed phase up to 20 wt.%. In the latter case, blends with a low viscosity ratio ($p < 1$) offer the best means towards a fine and stable phase morphology, unlike suggestions in the literature. Blends containing higher concentrations of the minor phase suffer seriously from coalescence effects; the influence of the viscosity ratio on the final blend phase morphology becomes less obvious, and the finest dispersion was observed at viscosity ratios around unity.

A quiescent thermal treatment of the blends showed that the concentration of the dispersed phase is the most important factor determining phase coarsening in blends having nearly equal melt-viscosities and melt-elasticities. Blending a highly viscous component with a low viscous component seems to counteract quiescent phase coarsening, even at higher concentrations of the dispersed phase, and hence offers an alternative towards both fine and relatively stable blend phase morphologies.

Acknowledgements

The authors are indebted to the Dow Benelux N.V. company for the financial support of this project, and to Marc Mangnus for the rheological measurements in plate-plate geometry. Profs. Mewis and Moldenaers (KU Leuven, Department of Chemical Engineering) are acknowledged for their support in the capillary rheometry experiments. The authors are also indebted to the Research Council KU Leuven and the Fund for Scientific Research Flanders (FWO-Vlaanderen).

References

- [1] Paul DR, Barlow JW. *J Macromol Sci-Rev Macromol Chem* 1980;C18:109.
- [2] Fortelný I, Cerná Z, Binko J, Ková J. *J Appl Polym Sci* 1993;48:1731.
- [3] Utracki LA, Shi ZH. *Polym Eng Sci* 1992;32:1824.
- [4] Elmendorp JJ. In: Rauwendaal C, editor. *Mixing in Polymer Processing*. New York: Marcel-Dekker, 1991.
- [5] Janssen JMH. PhD Thesis, TU Eindhoven, The Netherlands, 1993.
- [6] Taylor GI. *Proc Roy Soc* 1934;A146:501.
- [7] Grace HP. *Chem Eng Commun* 1982;14:225.
- [8] Wu S. *Polym Eng Sci* 1987;27:342.
- [9] Sundararaj U, Macosko CW. *Macromolecules* 1995;28:2647.
- [10] Elmendorp JJ, van der Vegt AK. *Polym Eng Sci* 1986;26:1332.
- [11] Fortelný I, Zivnů A. *Polymer* 1995;36:4113.
- [12] Smoluchowski M. *Phys Z* 1916;17:557–585.
- [13] Smoluchowski M. *Z Phys Chem* 1917;92:129.
- [14] Lyngaae-Jørgensen J, Utracki LA. *Makromol. Chem. Macromol Symp* 1991;48/49:189.
- [15] Elmendorp JJ. PhD Thesis, TU Delft, The Netherlands (1986).
- [16] Fortelný I, Kovár J. *Polym Compos* 1988;9:119.
- [17] Fortelný I, Kovár J. *Eur Polym J* 1989;25:317.
- [18] Hietaoja PT, Holsti-Miettinen RM, Seppälä JV, Ikkala OT. *J Appl Polym Sci* 1994;54:1613.
- [19] Favis BD, Chalifoux JP. *Polym Eng Sci* 1987;27:1591.
- [20] Favis BD, Chalifoux JP. *Polymer* 1988;29:1761.
- [21] Favis BD, Therrien D. *Polymer* 1991;32:1474.
- [22] Plochocki AP, Dagli SS, Andrews RD. *Polym Eng Sci* 1990;30:741.
- [23] Vainio TP, Seppälä JV. *Polymers and Polymer Composites* 1993;1:427.
- [24] Ghodgaonkar PG, Sundararaj U. *Polym. Eng. Sci.* 1996;36:1656 (cf. Sundararaj U, SPE Retec Symposium on Polymer Alloys and Blends, Boucherville, Canada, October 1995, Proceedings, p. 365).
- [25] Namhata S, Guest MJ, Aerts LM. *J Appl Polym Sci*, 1999;71:311.
- [26] Everaert V, Groeninckx G. *European Symposium on Polymer Blends*, Maastricht, The Netherlands, May 1996, Extended Abstracts, 111.
- [27] Min K, White JL, Fellers JF. *Polym Eng Sci* 1984;24:1327.
- [28] Chen CC, White JL. *Polym Eng Sci* 1993;33:923.
- [29] Schultz AR, Gendron BM. *J Appl Polym Sci* 1972;16:461.
- [30] Prest WM, Porter RS. *J. Polym. Sci. Polym Phys* 1972;10:1639.
- [31] Everaert V, Groeninckx G, Aerts L, Pionteck J, Favis B, Moldenaers P, Mewis J. *Polymer*, 1998 (submitted).
- [32] Heidemeyer PKH. PhD Thesis, R.W.T.H. Aachen, Germany, 1990.
- [33] Pahl MH. *Praktische Rheologie der Kunststoff schmelzen und Lösungen*. Düsseldorf: VDI-Verlag, 1983.
- [34] Favis BD, Lavalée C, Derdouri A. *J Mat Sci* 1992;27:4211.
- [35] Berger W, Kammer HW, Kummerlöwe C. *Makromol Chem Suppl* 1984;8:101.
- [36] Scott CE, Joung SK. *SPE Retec Symposium on Polymer Alloys and Blends*, Boucherville, Canada, October 1995, Proceedings, p. 338.
- [37] Sundararaj U, Macosko CW, Shih C-K. *Polym Eng Sci* 1996;36:1769.
- [38] Sundararaj U. *Macromol Symp* 1996;112:85.
- [39] Elemans PHM. PhD Thesis, TU Eindhoven, The Netherlands, 1989.
- [40] Jordhamo GM, Manson JA, Sperling LH. *Polym Eng Sci* 1986;26:517.
- [41] Chen TH, Su AC. *Polymer* 1993;34:4826.
- [42] Quintens D, Groeninckx G, Guest M, Aerts L. *Polym Eng Sci* 1990;30:1474.
- [43] Favis BD, Willis JM. *J Polym Sci Polym Phys* 1990;B28:2259.
- [44] Dedecker K. PhD Thesis, KU Leuven, Belgium, 1998.
- [45] Berger W, Kammer HW. *Makromol Chem Macromol Symp* 1987;12:145.
- [46] Lyngaae-Jørgensen J, Andersen FE, Alla N. *Polymer Alloys III*. New York: Plenum, 1983.
- [47] Chapleau N, Favis BD. *J Mat Sci* 1995;30:142.
- [48] Pötschke P, Wallheinke K, Fritsche H, Stutz H. *J Appl Polym Sci* 1997;65:2217.
- [49] Oshinski AJ, Keskkula H, Paul DR. *Polymer* 1996;37:4891.
- [50] Van Gisbergen JGM, Meijer HEH. *J Rheol* 1991;35:63.
- [51] Cheng TW, Keskkula H, Paul DR. *J Appl Polym Sci* 1992;45:1245.
- [52] Schoolenberg TE, Daring F, Ingenbeek G. *Makromol Chem Macromol Symp* 1996;112:107.